Inelastic positron scattering in an electron gas

J. Oliva*
University of California at San Diego, La Jolla, California 92093
(Received 13 August 1979)

The positron inelastic scattering rate γ in an electron gas is calculated in the full positron energy range within the random-phase approximation (RPA) using the Green's-function approach. Both particle-hole pair and plasmon excitation are taken into account. It is found that, for positron energy E much less than the Fermi energy E_0, particle-hole scattering gives $\gamma \simeq E^2$, whereas, for E much greater than E_0, plasmon scattering dominates and $\gamma \simeq (1/E^{1/2}) \ln(E/E_0)$. Interestingly, the plasmon excitation threshold energy for the positron is found to be the same as that for an electron. These results for a positron are compared with those for an electron obtained by Quinn.

I. INTRODUCTION

The recent development of energy-resolved high-flux low-energy positron beams[1,2] has led to some interest in the possible use of positron diffraction as a means of studying metal surfaces. This would be akin to low-energy electron diffraction (LEED)[3] and would provide information complementary to that provided by LEED. In addition, positron-metal surface scattering phenomena are of some interest in their own right. For example, recent experimental investigation[4,5] of low-to-medium-energy positron-metal surface scattering has led to the remarkable discovery that a substantial fraction of incident positrons leave the surface as positronium atoms.

As with the case of LEED we expect that an accurate calculation of low-energy positron-metal scattering amplitudes would have to take account of the inelastic scattering by conduction electrons. This scattering is one of the most significant sources of broadening of sharp features in the reflection pattern. Furthermore, the understanding of the positronium formation process[6,7] requires knowledge of the mean depth of penetration of the incident positron. This is primarily determined by inelastic positron-conduction electron scattering.[8]

This paper presents results of a calculation of the inelastic positron-conduction electron scattering in metals over the full positron energy range. The many-body field-theoretic approach is used. In Sec. II a positron Green's function and proper self-energy are defined. The imaginary part of the latter, Σ_I, is directly related to the total collision rate of a positron in an electron gas. In Sec. III we obtain an explicit and manageable expression for Σ_I within the random-phase approximation. Two contributions to Σ_I are identified, one associated with particle-hole pair excitation and the other with plasmon excitation. These are evaluated in Secs. IV and V where useful analytic expressions are provided in the low- and high-energy limits. The plasmon excitation threshold is also discussed. Quantitative results for the total Σ_I and mean free path for various r_s over the whole positron energy range and a comparison between Σ_I of a positron and that of an electron, are given in Sec. VI.

II. POSITRON GREEN'S FUNCTION

We consider a uniform system of a large number, N of electrons moving in a uniform neutralizing background and a single positron, all interacting via the Coulomb force. The second quantized Hamiltonian for the system may be written in the Schrödinger picture as[9]

$$\hat{H} = \hat{H}_0 + \hat{H}_{\rm INT} \ , \tag{1a}$$

$$\hat{H}_0 = -\frac{1}{2m}\sum_{\alpha}\int \psi_\alpha^\dagger(\vec{x})\nabla_{\vec{x}}^2\psi_\alpha(\vec{x})\,d^3x - \frac{1}{2m}\sum_{\beta}\int \phi_\beta^\dagger(\vec{x})\nabla_{\vec{x}}^2\phi_\beta(\vec{x})\,d^3x \ , \tag{1b}$$

$$\hat{H}_{\rm INT} = \tfrac{1}{2}e^2\sum_{\alpha\beta}\int \psi_\alpha^\dagger(\vec{x})\psi_\beta^\dagger(\vec{x}')\frac{1}{|\vec{x}-\vec{x}'|}\times\psi_\beta(\vec{x}')\psi_\alpha(\vec{x})\,d^3x d^3x' - e^2\sum_{\alpha\beta}\int \psi_\alpha^\dagger(\vec{x})\psi_\alpha(\vec{x})\frac{1}{|\vec{x}-\vec{x}'|}\times\phi_\beta^\dagger(\vec{x}')\phi_\beta(\vec{x}')\,d^3x d^3x' \ , \tag{1c}$$

where $\psi_\alpha^\dagger(\vec{x})[\psi_\alpha(\vec{x})]$ are electron field operators which create (destroy) an electron of spin α at the position $\vec{x}$, and where $\phi_\alpha^\dagger(\vec{x})[\phi_\alpha(\vec{x})]$ are positron field operators which create (destroy) a positron of spin α at the position $\vec{x}$. m is the electron and positron mass and e is the magnitude of the electron charge.

We seek to calculate the lifetime of the positron quasiparticle states. To this end we introduce a positron Green's function $G_{\alpha\beta}(\vec{x}t, \vec{x}'t')$ appropriate to the description of propagation of a single positron in an electron gas and defined as follows:

$$G_{\alpha\beta}(\vec{x}t, \vec{x}'t') = \frac{-i_H\langle\Psi_0|T[\phi_{H\alpha}(\vec{x}t)\,\phi^{\dagger}_{H\beta}(\vec{x}'t')]|\Psi_0\rangle_H}{{}_H\langle\Psi_0|\Psi_0\rangle_H} \quad , \tag{2}$$

where $\phi_{H\alpha}(\vec{x}t)$ and $\phi^{\dagger}_{H\beta}(\vec{x}'t')$ are the Heisenberg positron field operators and where $|\Psi_0\rangle_H$ denotes the Heisenberg ground state of a uniform, fully interacting, N-electron gas. T denotes the Dyson chronological operator. In our case $G_{\alpha\beta}$ is of the form $G\delta_{\alpha\beta}$.

By going to the Lehmann representation[10] for the Fourier transform $G(\vec{k}, \omega)$ of $G(\vec{x},t,\vec{x}',t') = G(\vec{x} - \vec{x}', t - t')$ it is seen that the poles of $G(\vec{k}, \omega)$ in the ω plane occur at the exact values of the change in energy associated with the addition to an interacting electron gas originally in the ground state of a single positron such that the final system ends up with momentum $\vec{k}$. For example, when the interaction between the positron and the electron gas is set equal to zero we find

$$G_0(\vec{k}, \omega) = \frac{1}{\omega - E(k) + i\eta} \quad , \tag{3}$$

where $E(k) = k^2/2m$ is the free positron energy.

In light of the form Eq. (3) we are led in the standard fashion to the following quasiparticle approximation for the fully interacting G:

$$G(\vec{k}, \omega) \approx \frac{Z(k)}{\omega - [\tilde{E}(k) + i\Gamma(k)]} \quad , \tag{4}$$

where we have written the complex-valued quasiparticle energy $\mathcal{E}(k)$ in terms of its real and imaginary parts $\tilde{E}(k)$ and $\Gamma(k)$. $Z(k)$ is an unimportant function related to the strength of the quasiparticle state.

The quasieigenstates behave in time as $e^{-i\mathcal{E}(k)t}$. The probability density of the quasiparticle having initial excitation energy $\tilde{E}(k)$ will decay in time exponentially at a rate $\gamma(k)$ given by:

$$\gamma(k) = 2|\Gamma(k)| \quad . \tag{5}$$

For the quasiparticle concept to be useful the damping rate must be small compared to the excitation energy:

$$\Gamma(k) \ll \tilde{E}(k) \quad . \tag{6}$$

A straightforward application of the Feynman-Dyson perturbation expansion scheme for G using H_{INT} of Eq. (1c) as the perturbation will lead to a Dyson equation for G which involves a positron proper self-energy Σ:

$$G(\vec{k}, \omega) = \frac{1}{\omega - E(k) - \Sigma(k, \omega)} \quad . \tag{7}$$

Upon comparing Eqs. (4) and (7), we may relate the quasiparticle energy $\mathcal{E}(k)$ to the proper self-energy $\Sigma(k, \omega)$. Denoting the real and imaginary parts of Σ by Σ_R and Σ_I we have in the case of long-lived excitations ($Z(k) \approx 1$):

$$\tilde{E}(k) = E(k) + \Sigma_R(k, \mathcal{E}(k)) \quad , \tag{8a}$$

$$\Gamma(k) = \left[1 - \frac{d}{d\omega}\Sigma_R(k, \omega)|_{\omega=\mathcal{E}(k)}\right]^{-1} \Sigma_I(k, \mathcal{E}(k)) \quad . \tag{8b}$$

Our interest here is in the damping rate $2|\Gamma|$. We make the approximation in Eq. (8b):

$$\Gamma(k) \approx \Sigma_I(k, \mathcal{E}(k)) \quad . \tag{9}$$

This is certainly valid for large k since $\Sigma(k, \mathcal{E}(k)) \to 0$ for $k \to \infty$, and is likely to be valid for small k where $\Sigma_R(k, \mathcal{E}(k))$ should be relatively flat.[11]

III. APPROXIMATE EVALUATION OF Σ_I

We now evaluate the imaginary part of the positron proper self-energy in an electron gas within the random-phase approximation (RPA). By this it is meant that the proper self-energy is approximated by an infinite summation of bubble-type diagrams of the form shown in the following equation:

$\Sigma_{\text{RPA}} \equiv$ 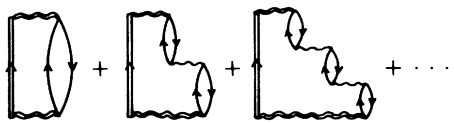 $+ \cdots$

$=$ 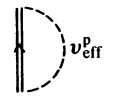 v^p_{eff} (10)

A double (single) simple line denotes a free positron (electron) Green's function; a double (single) wavy line denotes a bare positron-electron (electron-electron) Coulomb interaction. We have introduced with an obvious diagrammatic identification the effective interaction, v^p_{eff}, of a positron in an electron gas. These diagrams for $\Sigma(k, \omega)$ correspond to successive virtual excitations of electron particle-hole pairs by the positron. Through it it true, as with the case of electron RPA, that this approximation for Σ becomes very good (exact, in fact) only in the kinetic energy dominated high density limit $r_s \ll 1$,[12] we probably can expect qualitative, even semiquantitative validity for r_s in the metallic range $\sim 2 < r_s < \sim 5$.

We note that the exchange diagram (Fig. 1) appearing in the electron Σ_{RPA} has no analog here since there is only one positron in the system. Furthermore, since in all diagrams for v^p_{eff} there are exactly two electron-positron bare Coulomb interaction lines, each term is equal to the corresponding term in the

FIG. 1. Exchange contribution to electron self-energy.

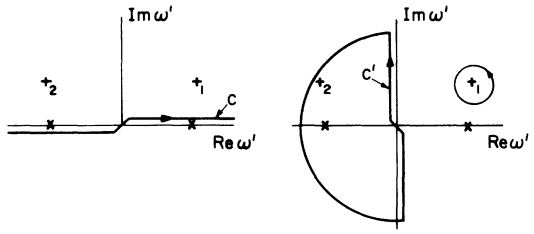

FIG. 2. Contours for self-energy evaluation. (a) Original contour C for the frequency integration. x denotes poles of dielectric function. + denotes a pole of the free positron Green's function. + occurs in the 1st quadrant when $\omega > E(\vec{p}-\vec{k})$, e.g., $+_1$, and it occurs in the 2nd quadrant when $E(\vec{p}-\vec{k}) > \omega$, e.g., $+_2$. Note from Eq. (15) that we are able to close the contour in, e.g., the upper half plane. (b) Rotate contour in (a) by $+90°$. A residue contribution arises when the pole + lies in the 1st quadrant. The contour C' may be now deformed into the imaginary axis.

electron effective potential, v^e_{eff}. We thus have

$$v^p_{\text{eff}}(k,\omega) = v^e_{\text{eff}}(k,\omega) - v(k) = v(k)\left[\frac{1}{\epsilon_{\text{RPA}}(k,\omega)} - 1\right] , \tag{11}$$

where $\epsilon_{\text{RPA}}(k,\omega)$ is the RPA (Lindhard) dielectric function of an N-electron gas [given below, Eq. (18)] and where $v(k)$ is the bare electron-electron Coulomb interaction:

$$v(k) = \frac{4\pi e^2}{k^2} . \tag{12}$$

The positron proper self-energy is given, in accordance with the Feynman rules, by:

$$\Sigma_{\text{RPA}}(p,\omega) = \frac{i}{(2\pi)^4}\int d^3k\, d\omega' G_0(\vec{p}-\vec{k},\omega-\omega') \times v^p_{\text{eff}}(k,\omega') , \tag{13}$$

which, using Eqs. (3) and (11), becomes

$$\Sigma_{\text{RPA}}(p,\omega) = \frac{i}{(2\pi)^4}\int d^3k \int_C d\omega' v(k)\left[\frac{1}{\epsilon_{\text{RPA}}(k,\omega')} - 1\right]\frac{1}{\omega-\omega'-E(\vec{p}-\vec{k})+i\eta} . \tag{14}$$

The frequency integral appearing in Eq. (14) is along the contour C (shown in Fig. 2), so chosen so as to properly avoid the poles of $\epsilon_{\text{RPA}}(k,\omega')$.

A rather convenient form for $\Sigma_{l,\text{RPA}}$ is now obtained (we from now on omit the subscript RPA on Σ_{RPA} and ϵ_{RPA}). Note the free-positron Green's function in the integrand of Eq. (14) has a pole at $\omega' = \omega_1 \equiv \omega - E(\vec{p}-\vec{k}) + i\eta$. Note further that since

$$\frac{1}{\epsilon(k,\omega')} - 1 \sim \frac{1}{|\omega'|^2}, \quad |\omega'| \to \infty , \tag{15}$$

we may close the contour C in Eq. (14) in the upper half plane. By rotating the resulting closed contour 90° counterclockwise [see Fig. 2(b)], we have

$$\Sigma(p,\omega) = \frac{i}{(2\pi)^4}\left[\int d^3k \int_{C'} d\omega' v(k)\left[\frac{1}{\epsilon(k,\omega')} - 1\right]\frac{1}{\omega-\omega'-E(\vec{p}-\vec{k})+i\eta} - 2\pi i\int_{0<E(\vec{p}-\vec{k})<\omega} d^3k\left[\frac{1}{\epsilon(k,\omega-E(\vec{p}-\vec{k})+i\eta)} - 1\right]v(k)\right] , \tag{16}$$

where C' is the $+90°$ rotated version of C. The second term in Eq. (16) arises from the fact that the pole of the free-positron propagator when in the first quadrant [i.e., when $\omega > E(\vec{p}-\vec{k})$] goes from being within to being outside the closed contour as C is rotated.

It can be shown that the imaginary part of the term involving the line integral in Eq. (16) vanishes.[13] We thus

arrive at the useful expression

$$\Sigma_I(p,\omega)=\frac{1}{(2\pi)^3}\,\mathrm{Im}\int_{0<E(\vec{p}-\vec{k})<\omega} d^3k\,\frac{v(k)}{\epsilon(k,\omega-E(\vec{p}-\vec{k})+i\eta)}\ , \tag{17}$$

which will serve as the starting point for the subsequent development.

The real and imaginary parts $\epsilon_r(k,\omega)$ and $\epsilon_i(k,\omega)$ of the Lindhard dielectric function are given by[14]:

$$\epsilon_r(k,\omega)=1+\frac{2me^2p_0}{\pi k^2}\left\{1-\frac{p_0}{2k}\left[1-\left(\frac{\omega m}{p_0k}-\frac{k}{2p_0}\right)^2\right]\ln\left|\left[1+\left(\frac{\omega m}{p_0k}-\frac{k}{2p_0}\right)\right]\Big/\left[1-\left(\frac{\omega m}{p_0k}-\frac{k}{2p_0}\right)\right]\right|\right.$$

$$\left.+\frac{p_0}{2k}\left[1-\left(\frac{\omega m}{p_0k}+\frac{k}{2p_0}\right)^2\right]\ln\left|\left[1+\left(\frac{\omega m}{p_0k}+\frac{k}{2p_0}\right)\right]\Big/\left[1-\left(\frac{\omega m}{p_0k}+\frac{k}{2p_0}\right)\right]\right|\right\}\ , \tag{18a}$$

$$\epsilon_i(k,\omega)=\begin{cases}\epsilon_{i1}=\dfrac{me^2p_0^2}{k^3}\left[1-\left(\dfrac{\omega m}{p_0k}-\dfrac{k}{2p_0}\right)^2\right], & \dfrac{k}{p_0}+\dfrac{1}{2}\left(\dfrac{k}{p_0}\right)^2\geqslant\dfrac{\omega m}{p_0^2}\geqslant\left|\dfrac{k}{p_0}-\dfrac{1}{2}\left(\dfrac{k}{p_0}\right)^2\right| \\ \epsilon_{i2}=\dfrac{2m^2e^2\omega}{k^3}, & \dfrac{k}{p_0}\leqslant 2,\quad 0\leqslant\dfrac{\omega m}{p_0^2}\leqslant\dfrac{k}{p_0}-\dfrac{1}{2}\left(\dfrac{k}{p_0}\right)^2\end{cases}\ , \tag{18b, 18c}$$

where p_0 is the Fermi momentum of the electron gas

$$p_0=(3\pi^2n)^{1/3}\ , \tag{19}$$

n being the electron density.

It will be seen that there are in general two types of contributions to Σ_I [see Eq. (17)]: one from the integration over the region of $\vec{k}$ space where $\epsilon_i(k,\omega-E(\vec{p}-\vec{k})+i\eta)$ is finite (this corresponding to the positron's exciting particle-hole pairs) and the other arising from any poles in the integrand (i.e., zeros of ϵ) falling within the domain of integration (this corrsponding to the positron's exciting plasmons).

We take for the approximate collision rate $2|\Gamma|$ [see Eq. (9)] twice the value of the imaginary part of the self-energy $\Sigma_I(p,\mathcal{E}(p))$, evaluated at frequency $\mathcal{E}(p)=E(p)$, i.e., the on-shell value. We will thus be evaluating

$$\Sigma_I(p)=\frac{1}{(2\pi)^3}\,\mathrm{Im}\int_{0<E(\vec{p}-\vec{k})<E(p)} d^3k\times\frac{v(k)}{\epsilon(k,E(p)-E(\vec{p}-\vec{k})+i\eta)} \tag{20}$$

IV. PARTICLE-HOLE CONTRIBUTION

As indicated in Eq. (18), the imaginary part of the dielectric function $\epsilon(k,\omega)$ is nonzero when either $p_0k+\frac{1}{2}k^2\geqslant m\omega\geqslant|p_0k-\frac{1}{2}k^2|$, or $k\leqslant 2p_0$ and $0\leqslant m\omega\leqslant kp_0-\frac{1}{2}k^2$. Using the fact that in the integral of Eq. (20), $\epsilon(k,\omega)$ enters with frequency argument $\omega=(1/2m)(2pk\cos\theta-k^2)$ (θ is the angle between $\vec{p}$ and $\vec{k}$), it is straightforward to show that this set of inequalities reduces to the one simple inequality:

$$|k-p\cos\theta|\leqslant p_0\ . \tag{21}$$

The region of $\vec{k}$ space specified by this inequality is bounded by a surface known as a Pascal limacon of revolution. For $p>p_0$, there are two branches of the surface (one contained in the other) whereas for $p<p_0$, there is a single branch [Fig. 3]. The region of $\vec{k}$ space in which

$$\mathrm{Im}\epsilon\left(k,\frac{1}{2m}(2pk\cos\theta-k^2)\right)$$

is nonzero and which contributes to the integral Eq. (20) is then the region which is both within the Pascal limacon (when $p>p_0$ this means between the two branches) and within the sphere of radius p cen-

tered at $\vec{k}=\vec{p}$ [Fig. 3]. We have then for the particle-hole contribution,

$$\Sigma_{l_{\rm ph}}(p)=\begin{cases}\dfrac{e^2}{\pi}\,\mathrm{Im}\displaystyle\int_0^1 dx\int_0^{2px} dk\,\frac{1}{\epsilon_r(k,(1/2m)(2pkx-k^2))+i\epsilon_{i_2}(k,(1/2m)(2pkx-k^2))}, & p<p_0\ . \quad (22a)\\[2ex] \dfrac{e^2}{\pi}\,\mathrm{Im}\left[\displaystyle\int_0^{p_0/p} dx\int_0^{2px} dk\,\frac{1}{\epsilon_r(k,(1/2m)(2pkx-k^2))+i\epsilon_{i_2}(k,(1/2m)(2pkx-k^2))}\right. & \\ \qquad\left.+\displaystyle\int_{p_0/p}^1 dx\int_{px-p_0}^{px+p_0} dk\,\frac{1}{\epsilon_r(k,(1/2m)(2pkx-k^2))+i\epsilon_{i_1}(k,(1/2m)(2pkx-k^2))}\right], & p>p_0\ . \quad (22b)\end{cases}$$

We first consider the case $p \ll p_0$. Entering into Eq. (22a) is then the dielectric function evaluated for momentum and energy very small compared to p_0 and the Fermi energy $E_0=p_0^2/2m$, respectively:

$$\epsilon\left(k,\frac{1}{2m}(2pk\cos\theta-k^2)\right)\approx\frac{4me^2p_0}{\pi k^2}+i\frac{me^2}{k^2}(2p\cos\theta-k)\ . \quad (23)$$

We readily arrive at

$$\Sigma_{l_{\rm ph}}(p)\approx-\frac{\pi p_0^2}{60m}\left(\frac{p}{p_0}\right)^4\sim r_s^2p^4;\quad p\ll p_0\ . \quad (24)$$

We see that the collision rate tends to zero as $p\to 0$, this reflecting the decreasing phase space available to the scattered electrons as the energy transfer tends to zero. We note that in this small momentum regime the particle-hole contribution to the collision rate decreases with increasing electron density. This is consistent with the fact that at higher densities, where the kinetic energy dominates the dynamics, the electrons are less able to respond to the presence of an external charge.

We now consider the case of high momentum $p \gg p_0$. Starting with Eq. (22b) it can be shown that for this range of p, $\Sigma_{l_{\rm ph}}(p)$ varies inversely with p:

$$\Sigma_{l_{\rm ph}}(p)\approx\frac{p_0}{p}C(p_0),\quad p\gg p_0. \quad (25a)$$

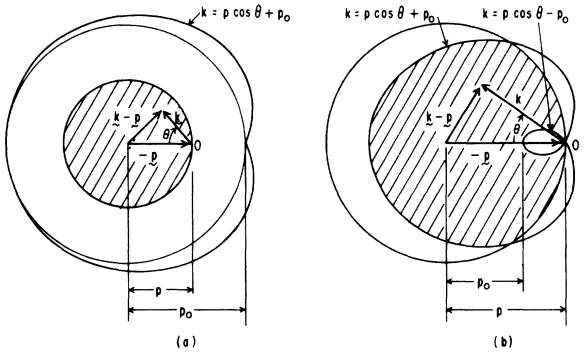

FIG. 3. Cross section of region of $\vec{k}$ space contributing to $\Sigma_{l_{\rm ph}}(p)$. (a) $p<p_0$; (b) $p>p_0$. 0 is the origin of $\vec{k}$ space. Shaded regions correspond to points $\vec{k}$ lying both within the domain of integration in Eq. (20) (within the sphere of radius p centered at $\vec{k}=\vec{p}$) and within the region of $\vec{k}$ space in which $\mathrm{Im}\epsilon(k,(1/2m)(2pk\cos\theta-k^2))\neq 0$.

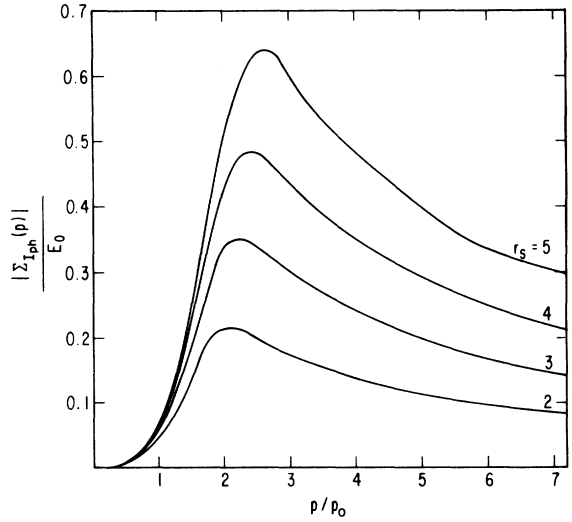

FIG. 4. Particle-hole contribution to imaginary part of self-energy vs momentum.

with

$$C(p_0)=\frac{e^2}{\pi}\,\mathrm{Im}\left[\int_1^\infty du\int_{p_0(u-1)}^{p_0(u+1)}dk\frac{1}{\epsilon_r(k,(1/2m)(2p_0ku-k^2))+i\epsilon_{i_1}(k,(1/2m)(2p_0ku-k^2))}\right.$$
$$\left.+\int_0^1 du\int_0^{2p_0u}dk\frac{1}{\epsilon_r(k,(1/2m)(2p_0ku-k^2))+i\epsilon_{i_2}(k,(1/2m)(2p_0ku-k^2))}\right]. \tag{25b}$$

We present plots of $|\Sigma_{I_{\rm ph}}(p)/E_0|$ vs p/p_0 for various r_s (Fig. 4). For intermediate momenta we have resorted to numerical integration. The results show that the p^4 dependence for small p is valid up to $\sim 0.1p_0$. Increasing p further, the curves rise somewhat rapidly to a relatively broad maximum at $p\sim 2p_0$ [with values of $|\Sigma_{I_{\rm ph}}(p)/E_0|$ at the maximum ranging from ~ 0.5 for $r_s=4$ to ~ 0.2 for $r_s=2$] and then fall rather slowly. We found that the $1/p$ variation for $p>>p_0$ becomes discernible for $p>\sim 20p_0$.

V. PLASMON CONTRIBUTION

As noted earlier, the plasmon contribution to $\Sigma_I(p)$ arises when the pole of $\epsilon^{-1}(k,E(k)-E(\vec{p}-\vec{k})+i\eta)$ falls within the domain of integration [Eq. (20)]. The plasmon excitation energy $\omega_p(k)$ solves the equation of the longitudinal resonance condition: $\epsilon(k,\omega_p(k))=0$. The plasmon excitation spectrum starts at $k=0$ with energy ω_0 given by

$$\omega_0=\left[\frac{4\pi ne^2}{m}\right]^{1/2}, \tag{26}$$

rises to a maximum value $\omega_p(k_c)$ at the plasmon cutoff momentum k_c, and ceases to be a well-defined excitation for $k>k_c$. The cutoff is determined by the condition that it becomes possible for a plasmon to decay into a single pair excitation, i.e., when

$$\frac{k^2}{2m}+\frac{kp_0}{m}=\omega_p(k)\ . \tag{27}$$

From Eq. (20) and the comment above, we see that the poles of the inverse dielectric function are encountered during the k integration for $\Sigma_I(p)$ when both

$$E(p)-E(\vec{p}-\vec{k})=\omega_p(k) \tag{28a}$$

and

$$k<k_c\ . \tag{28b}$$

We neglect the small dispersion of the plasmon mode and set

$$\omega_p(k)=\omega_0\ . \tag{29}$$

Then the conditions (28) for a pole become

$$\frac{1}{2m}(p^2-|\vec{p}-\vec{k}|^2)=\omega_0\ , \tag{30a}$$

$$k<k_c^0\ , \tag{30b}$$

with the cutoff momentum in the absence of dispersion, k_c^0 given by:

$$k_c^0=(p_0^2+2m\omega_0)^{1/2}-p_0\ . \tag{31}$$

The set of points $\vec{k}$ satisfying Eq. (30a) is a sphere centered at $\vec{k}=\vec{p}$ and of radius $(p^2-2m\omega_0)^{1/2}$. When $(p^2-2m\omega_0)^{1/2}<p_0$, points $\vec{k}$ on this sphere are such that $k>k_c^0$, and thus do not satisfy the second requirement for a pole, Eq. (30b). There then is no plasmon contribution to $\Sigma_I(p)$ in this case.

On the other hand, for radius $(p^2-2m\omega_0)^{1/2}>p_0$, the sphere of points satisfying Eq. (30a) does at least pass through regions of the domain of integration in which $\mathrm{Im}\epsilon(k,E(p)-E(\vec{p}-\vec{k})+i\eta)=0$, namely, referring to Fig. 5(b), the crescent-shaped region bounded by both the outer branch of the Pascal lima-

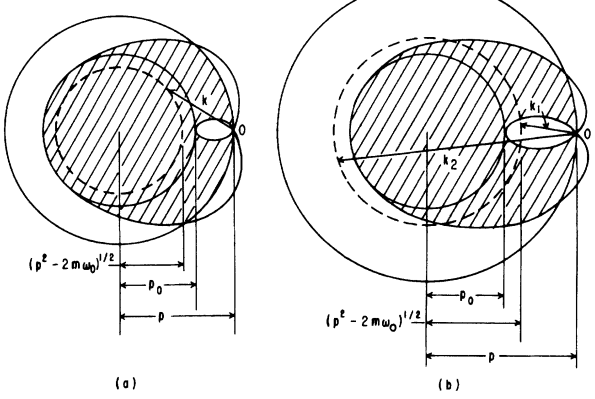

FIG. 5. (a), (b) Plasmon-contribution to $\mathrm{Im}\Sigma(p)$. The energy conservation condition $\omega_p(k)=E(p)-E(\vec{p}-\vec{k})$ is satisfied for $\vec{k}$ on dotted spheres in both cases. Only when its radius is greater than p_0 do points on this sphere lie in regions where (b) $\mathrm{Im}\epsilon(k,(1/2m)(2pk\cos\theta-k^2))=0$ and then, only points such as k_1, in the small oval give a zero of $\epsilon(k,(1/2m)\times(2pk\cos\theta-k^2))$. [$\mathrm{Re}\epsilon(k,(1/2m)(2pk\cos\theta-k^2))\neq 0$ for points such as k_2.] Obviously, threshold corresponds to the p for which the dotted sphere coincides with the sphere centered at $\vec{k}=\vec{p}$, and of radius p_0.

con and the sphere of radius p, and the oval region bounded by the inner branch of the limacon. Only in the oval region, however, do the points on the sphere also satisfy the additional condition for a pole, Eq. (30b) [$\mathrm{Re}\epsilon(k, E(p) - E(\vec{p} - \vec{k}) + i\eta) \neq 0$ in the crescent region], and it is therefore from only this region that we get a plasmon contribution to $\Sigma_I(p)$.

We conclude that the value of positron momentum at the threshold for excitation of a plasmon is, neglecting dispersion, given by

$$p_{\mathrm{th}} = (2m\omega_0 + p_0^2)^{1/2} \ . \tag{32}$$

The same value of plasmon excitation threshold momentum was found by Quinn[15] (again neglecting dispersion) for the case of an electron probe interacting with an electron gas. One might offhand say that the value p_{th} is reasonable for the electron case since the external electron cannot, after exciting a plasmon, end up with an energy less than E_0, the corresponding states already being occupied. This line of reasoning would seem to lead to the following "paradox." For a positron scattering from an electron gas, one is then tempted to say that the plasmon excitation threshold should occur at $E(p) = \omega_0$, with the scattered positron, ending up in the $E(p) = 0$ state.

The discrepancy suggested by the last argument lies of course in its failing to take account of the implications of momentum conservation. If a positron of energy $E(p) = \omega_0$ were to excite a plasmon, it would have to give up a momentum $(2m\omega_0)^{1/2}$. But this is in excess of the plasmon cutoff momentum $k_c^0 = (p_0^2 + 2m\omega_0)^{1/2} - p_0$, therefore implying that such a positron is after all unable to excite a plasmon.

Note in fact that at the actual threshold p_{th} [Eq. (32)] the plasmon excited will have momentum equal to the cutoff momentum k_c^0. As positron momentum is increased above p_{th}, it will be able to excite plasmons with momenta ranging from a low of $k_{\mathrm{min}} = p - (p^2 - 2m\omega_0)^{1/2}$ (forward scattering) to a high of k_c^0 [the positron scattering at an angle $\cos^{-1}(p_0/p)$ from its original direction]. These statements follow simply from Figs. 5(a) and 5(b). Note that k_{min} tends to zero as p tends to infinity.

For $p > p_{\mathrm{th}}$ we thus have a plasmon contribution to $\Sigma_I(p)$ which we denote by $\Sigma_{I_{\mathrm{pl}}}(p)$, and which is given by

$$\Sigma_{I_{\mathrm{pl}}}(p) = \frac{1}{(2\pi)^3} \int_{\mathrm{oval}} d^3k \, \mathrm{Im} \frac{v(k)}{\epsilon(k, E(p) - E(\vec{p} - \vec{k}) + i\eta)}, \quad p > p_{\mathrm{th}} \ . \tag{33}$$

In the oval region we approximate the dielectric function by its high frequency, low wave vector form (i.e., again neglecting dispersion):

$$\epsilon(k, \omega) \approx 1 - \omega_0^2/\omega^2 \ . \tag{34}$$

Upon using Eq. (34) in Eq. (33), introducing spherical coordinates with $\vec{p}$ taken along the polar axis, we eventually find

$$\Sigma_{I_{\mathrm{pl}}}(p) = -\frac{me^2\omega_0}{2p} \ln \left| \frac{(p_0^2 + 2m\omega_0)^{1/2} - p_0}{p - (p^2 - 2m\omega_0)^{1/2}} \right| , \tag{35}$$

$p > p_{\mathrm{th}}$.

We remark that precisely the same result was obtained for the plasmon contribution to the imaginary part of the electron self-energy in an electron gas by Quinn.[16] Though this is consistent with our earlier observation of the equality of the positron and electron plasmon excitation threshold momenta, the equality of the two self-energy contributions is slightly surprising. For $p \gg p_0$ we find

$$\Sigma_{I_{\mathrm{pl}}}(p) \approx -\frac{me^2\omega_0}{2p} \ln \left| \frac{p}{p_0} \right| . \tag{36}$$

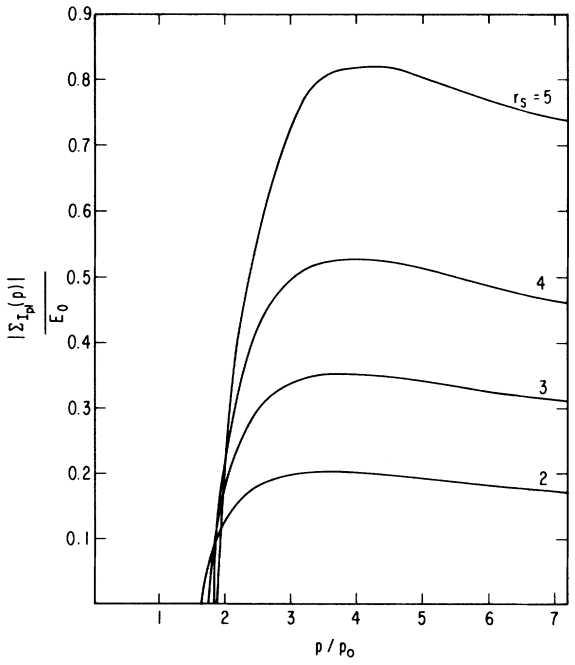

FIG. 6. Plasmon contribution to imaginary part of self-energy vs momentum.

In view of Eqs. (25) and (36), we conclude that the total collision rate of a fast positron moving in an electron gas decreases with increasing momentum. Moreover, comparing Eqs. (25) and (36) we see that the plasmon contribution to the collision rate dominates at high momentum. Thus,

$$\gamma(p) \approx \frac{me^2\omega_0}{p} \ln\left(\frac{p}{p_0}\right), \quad \frac{p}{p_0} \to \infty \ . \tag{37}$$

Finally, we present plots of $|\Sigma_{I_{pl}}(p)/E_0|$ vs p/p_0 for relevant r_s (Fig. 6).

VI. TOTAL COLLISION RATE AND MEAN FREE PATH

The total value for $\Sigma_I(p)$ is given by the sum $\Sigma_{I_{ph}}(p) + \Sigma_{I_{pl}}(p)$ [Eqs. (22) and (35)]. Before proceeding to a discussion of the character of $\Sigma_I(p)$ it is necessary that we verify the notion implicit until this point that the probe interacting with the electron gas forms a reasonably well-defined quasiparticle state. More precisely put, we must verify that the energy width of our quasieigenstates, namely $\Sigma_I(p)$ is small compared to the excitation energy $E(p)$. Plots of $|\Sigma_I(p)/E(p)|$ vs p/p_0 are presented in Fig. 7 for representative r_s. It is seen that only rarely does this ratio approach even a tolerable $\sim 20\%$. For the most part, the fractional uncertainty is considerably smaller. We can be assured then that our results are reasonably sensible.

We are now able to present the following picture for the RPA total collision rate of a positron moving through an electron gas. Plots of $|\Sigma_I(p)/E_0| = \frac{1}{2}\gamma/E_0$ vs p/p_0 appear in Fig. 8 for relevant r_s. For $p < p_0$, only particle-hole pairs are excited. $|\Sigma_I(p)|$ starts off with a $\sim p^4 r_s^2$ dependence and increases smoothly through the region $p \approx p_0$. At a

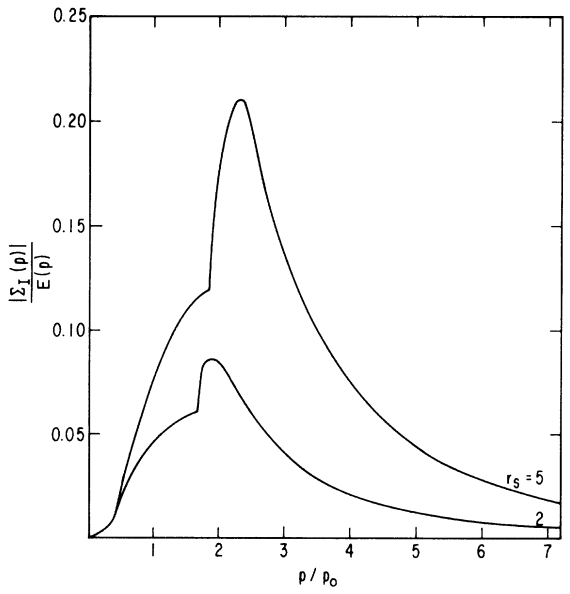

FIG. 7. Quasiparticle fractional uncertainty vs momentum.

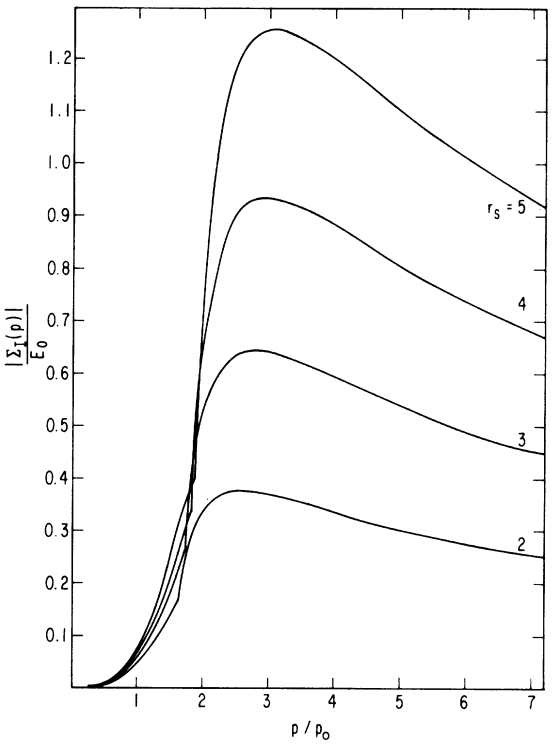

FIG. 8. Imaginary part of self-energy vs momentum.

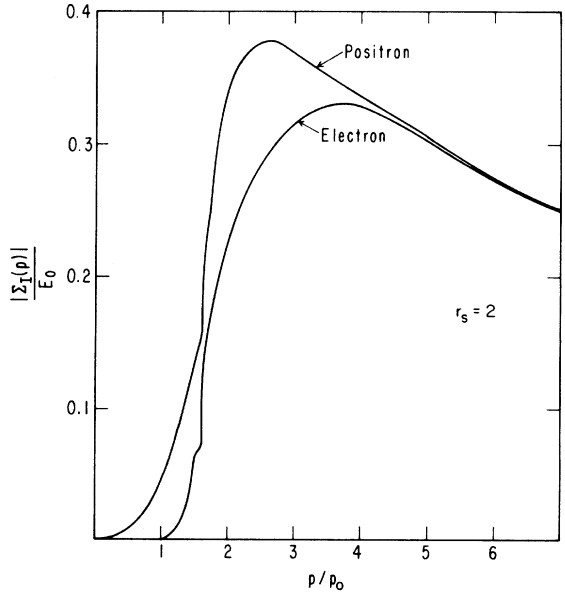

FIG. 9. Comparison between imaginary parts of electron and positron self-energy.

momentum $p = p_{th} \sim 2p_0$ (for r_s of interest) the positron begins to excite plasmons (in addition to ph pairs), this being manifested in a nonanalytic rise in $|\Sigma_I(p)|$ there. There is then a rather broad maximum, of magnitude ranging from $\sim 0.4E_0$ for $r_s = 2$ to $\sim 0.9E_0$ for $r_s = 4$, reached at $p \sim 2-4p_0$. This is followed by a relatively slow dropoff with an asymptotic $\sim (1/p)\ln(p/p_0)$ dependence, originating from the dominating plasmon excitation channel.

In Fig. 9 we present a comparison between our result for $\Sigma_I(p)$ for a positron and Quinn's results for the same for an electron. The larger magnitude of the imaginary part of the positron self-energy is readily understood: since the positron does not see the Pauli restrictions operative for the electron, it has more available phase space to scatter into, resulting in its having a higher collision rate.

The mean free path $\lambda(p)$ of a positron quasiparticle with excitation energy $\tilde{E}(p)$ may be taken as

$$\lambda(p) = \frac{d}{dp}\tilde{E}(p)\frac{1}{\gamma(p)} \quad . \tag{38}$$

Now $\tilde{E}(p)$ is given approximately by Eq. (8a). We will here ignore the p dependence of $\Sigma_R(p, \delta(p))$ and take simply

$$\lambda(p) \approx \frac{p}{m}\frac{1}{\gamma(p)} \quad . \tag{39}$$

A plot of $\lambda(E)$ vs E appears in Fig. 10. The correspondence between the structure in Σ_I described above and that in λ is apparent

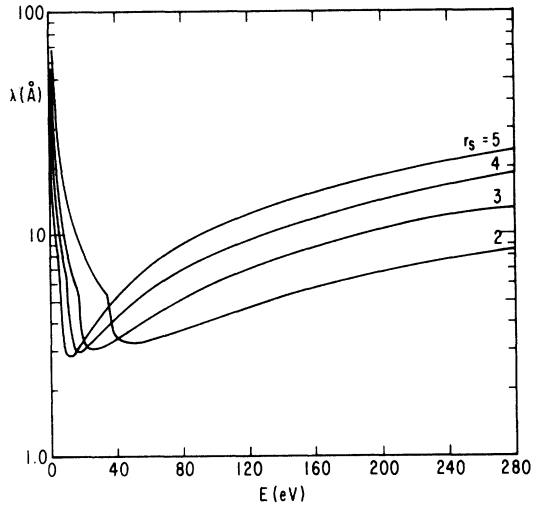

FIG. 10. Mean free path vs energy.

$$\lambda(E) \approx \begin{cases} \dfrac{15\sqrt{2}E_0}{\pi e^2 a_0 m^{3/2}}\dfrac{1}{E^{3/2}}, & E \ll E_0 \ , \qquad (40) \\ \dfrac{4}{me^2\omega_0}\dfrac{E}{\ln(E/E_0)}, & E \gg E_0 \ . \qquad (41) \end{cases}$$

A minimum of the order of a few angstroms occurs at $E \sim 2E_0$.

The author wishes to thank Professor W. Kohn for numerous helpful discussions. The support of ONR (Contract No. N00014-76-C) is gratefully acknowledged.

---

*Present address: Laboratory of Atomic and Solid State Physics, Cornell University, Ithaca, N.Y. 14853.

[1]K. F. Canter, A. P. Mills, Jr., and S. Berko, Phys. Rev. Lett. 33, 7 (1974).

[2]T. S. Stein, W. E. Kauppila, and L. O. Roellig, Phys. Lett. A 51, 327 (1975), and references cited therein.

[3]Referred to as "LEPD" by some.

[4]Canter, Mills, and Berko, Ref. 1.

[5]A. P. Mills, Jr., Phys. Rev. Lett. 41, 1828 (1978).

[6]Mills, Ref. 5.

[7]J. Oliva, Ph.D. thesis (University of California at San Diego, 1979) (unpublished).

[8]J. Olivia, Phys. Rev. B 21, 4918 (1980) (following paper).

[9]We set $\hbar = 1$ throughout.

[10]A. A. Abrikosov, L. P. Gorkov, and I. E. Dzyaloshinskii, *Methods of Quantum Field Theory in Statistical Physics* (Prentice-Hall, Engelwood Cliffs, 1963), Sec. 7.

[11]$\Sigma_R(k, \delta)$ is essentially the positron correlation energy in the electron gas arising from the screening response of the electrons. The screening is expected to be relatively insensitive to variations in positron energy well below the Fermi energy E_0.

[12]$r_s = (3/4\pi n)^{1/3}(1/a_0)$, where n is the electron density and a_0 is the Bohr radius.

[13]After replacing C' by the imaginary axis and setting $\eta = 0$, introduce the change of variables $u = i\omega'$. Noting that $\epsilon(k, \omega')$ has the symmetry property $\epsilon(k, \omega') = \epsilon(k, -\omega')$, the resulting integral is manifestly real.

[14]A. L. Fetter and J. D. Walecka, *Quantum Theory of Many Particle Systems* (McGraw-Hill, New York, 1971), Sec. 12.

[15]J. J. Quinn, Phys. Rev. 126, 1453 (1962).

[16]Quinn, Ref. 15.